DE GRUYTER

Chapter for Handbook of Fractional Calculus with Applications

James F. Kelly and Mark M. Meerschaert*

The fractional advection-dispersion equation for contaminant transport

DOI ...

Abstract: Anomalous dispersion is observed throughout hydrology, yielding a contaminant plume with heavy leading tails. The fractional advection dispersion equation (FADE) captures this behavior by replacing the second-order spatial derivative with a Riemann-Liouville (RL) fractional derivative. The RL fractional derivative is a nonlocal operator and models large jumps of solute particles in heterogeneous media. This chapter reviews the FADE, including fundamental (point-source) solutions, which are expressed as stable probability density functions. The space FADE has been extended to space-dependent parameters (e.g., dispersivity) and multiple dimensions. Alternatively, the time FADE and fractional mobile immobile (FMIM) models, which utilize time-fractional derivatives to model long-waiting times (retention), are also used to model anomalous dispersion. Current applications of the FADE, including parameter estimation, source identification, space-time duality, and FADE models on bounded domains are discussed.

Keywords: Fractional dispersion, continuous time random walks, parameter fitting, source identification, space-time duality

PACS: ...

1 Introduction

Non-Fickian, or anomalous, dispersion is observed throughout hydrology in both surface [2, 25, 32, 53] and subsurface [9, 11, 19, 62] flows through heterogeneous porous media. Solute particles may experience long movements due to high-velocity preferential flow paths, yielding a particle plume with heavy leading

James F. Kelly, Department of Statistics and Probability, Michigan State University, East Lansing, Michigan, USA
***Corresponding author: Mark M. Meerschaert,** Department of Statistics and Probability, Michigan State University, East Lansing, Michigan, USA

tails. As a result, the solute spreads in a super-diffusive manner. The traditional advection dispersion equation (ADE) with constant coefficients cannot model this feature of anomalous dispersion. To address this problem, the fractional advection dispersion equation (FADE) was introduced in Benson et al. [7–9], replacing the second derivative in space with a fractional Riemann-Liouville (RL) derivative. Thus, the FADE introduces *spatial nonlocality* [20, 21, 24], using an integro-differential operator with a power-law kernel, to model a wide range of flow velocities.

The FADE has successfully modeled tracer tests in underground aquifers, including the MADE tracer tests in a highly heterogeneous aquifer located on a US Air Force base in Mississippi [9, 12, 17], tracer tests in the Cape Code sand and gravel aquifer [7], unsaturated soils [65], saturated porous media [73], streams and rivers [1, 25, 27], and overland solute transport due to rainfall [26]. More recently, the FADE has modeled anomalous mixing and reaction between multiple chemical species [13, 14]. Some of this success may be attributed to the simplicity of the FADE: a wide range of observed behavior in heterogeneous media is captured with a parsimonious model with just four parameters.

This chapter focuses on the spatial FADE in both 1D and multiple dimensions. In Section 2, we first discuss the one-dimensional FADE. We then discuss variants of the FADE with variable coefficients. Fundamental solutions to the FADE with constant coefficients are expressed in terms of a *stable* probability density function. In Section 3, we describe the multi-dimensional FADE [40]. Section 4 briefly surveys two time-fractional models: the time FADE [63] and the fractional mobile-immobile model (FMIM) [58]. Section 5 examines two inverse problems associated with the FADE: parameter estimation and source identification. Finally, current research and unsolved problems are discussed in Section 6.

2 The Fractional Advection-Dispersion Equation

The 1D space-fractional advection dispersion equation (FADE) for concentration $C(x,t)$ [M/L^3] with *constant coefficients* is given by

$$\frac{\partial C}{\partial t} + v\frac{\partial C}{\partial x} = D\frac{1+\beta}{2}\frac{\partial^\alpha C}{\partial x^\alpha} + D\frac{1-\beta}{2}\frac{\partial^\alpha C}{\partial(-x)^\alpha}, \tag{1}$$

where v [L/T] is the average plume velocity, D [L$^\alpha$/T] is a fractional dispersion coefficient that controls the rate of spreading, $1 \le \alpha \le 2$ (dimensionless) and $-1 \le \beta \le 1$ (dimensionless) is the skewness parameter. The first and second terms on the right hand of (1) are the positive (left) and negative (right) *Riemann-Liouville* (RL) fractional derivatives. If $\beta = 1$, then solutions to the FADE are positively-skewed, while if $\beta = -1$, solutions are negatively skewed. If $\beta = 0$, the sum of the two RL fractional derivatives is equivalent to the symmetric *Riesz* derivative, and the resulting solution is symmetric. The fractional order α codes for the heterogeneity of the velocity field, with a higher probability of large velocities as α decreases towards one, see Clarke et al. [17].

If $\alpha = 2$, the FADE reduces to the traditional advection-dispersion equation (ADE) for groundwater flow and transport (e.g., see Bear [6]). The FADE (1) was introduced by Benson et al. [8] to model scale-dependent dispersivity in fitted groundwater plumes, i.e., the fact that the fitted parameter D grows with time when the ADE is applied to data. Such evidence of superdiffusion is an indicator that a space-fractional model may be preferable. Indeed, Benson et al. [7–9] show that the FADE (1) with $1 < \alpha < 2$ allows the same data to be fit with a constant coefficient model, where D does not vary over time.

The positive and negative RL derivatives in (1) may be computed using the (shifted) *Grünwald-Letnikov* finite difference formula introduced by Meerschaert and Tadjeran [46]:

$$\frac{\partial^\alpha C}{\partial x^\alpha} = \lim_{h\to 0} h^{-\alpha} \sum_{j=0}^{\infty} g_j^\alpha C\left(x-(j-1)h, t\right) \tag{2a}$$

$$\frac{\partial^\alpha C}{\partial (-x)^\alpha} = \lim_{h\to 0} h^{-\alpha} \sum_{j=0}^{\infty} g_j^\alpha C\left(x+(j-1)h, t\right), \tag{2b}$$

where the Grünwald weights g_j^α are given by

$$g_j^\alpha = (-1)^j \frac{\Gamma(\alpha+1)}{\Gamma(j+1)\Gamma(\alpha-j+1)} = \frac{-\alpha(1-\alpha)\cdots(j-1-\alpha)}{j!}.$$

From these definitions, we see that the RL fractional derivative is a nonlocal operator: the change in concentration at position x does not just depend on nearby locations, but distant locations as well. From a particle perspective, a combination of positive and negative RL derivatives allows a solute particle to *jump* to any point in the domain. Figure 1 illustrates this situation, and Schumer et al. [57] provide a derivation of (1) using this Eulerian particle picture. In brief, the FADE models contaminant transport through a heterogeneous porous medium, using a nonlocal fractional derivative that captures a highly variable velocity field.

The FADE (1) governs the long-time limit of a random walk with long-tailed particle jumps, and $C(x, t)$ is the probability density function (PDF) of the

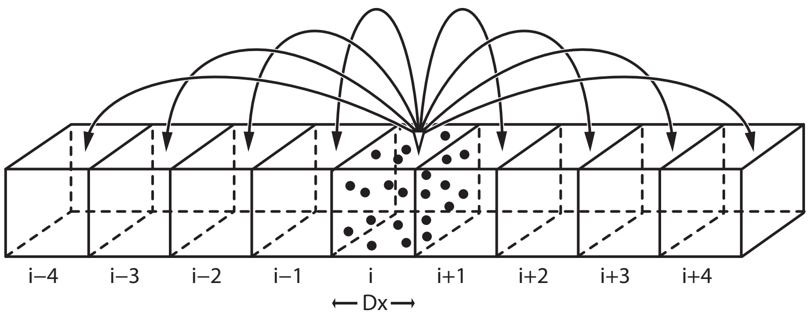

Fig. 1: Fractional diffusion of particles between distant cells, illustrating the nonlocality of the RL fractional derivative, from [57].

limiting stochastic process. Suppose that (X_n) are independent and identically distributed (IID) random variables that represent the particle jumps, and $S_n = X_1 + \cdots + X_n$ is a random walk that represents the position of a randomly selected particle after the nth jump. Suppose that $\mathbb{P}[X_n > x] = pCx^{-\alpha}$ and $\mathbb{P}[X_n < -x] = qCx^{-\alpha}$ for some $C > 0$ and $1 < \alpha < 2$, where p, q are nonnegative constants such that $p + q = 1$. Then the mean $v = \mathbb{E}[X_n]$ exists and we have

$$n^{-1/\alpha} \sum_{j=1}^{[nt]} (X_j - v) + n^{-1} \sum_{j=1}^{[nt]} v \Rightarrow Z_t + vt, \tag{3}$$

where Z_t is a stable Lévy motion with mean zero [44, Remark 4.17]. The PDF $C(x,t)$ of $Z_t + vt$ solves the FADE (1) with $D = C\Gamma(2-\alpha)/(\alpha-1)$ and $\beta = p-q$ [44, Proposition 4.16]. If X_n are IID with a finite variance $\sigma^2 = \mathbb{E}[(X_n - v)^2]$, then (3) holds with $\alpha = 2$, Z_t is a Brownian motion, and $C(x,t)$ solves the FADE (1) with $\alpha = 2$ and $D = \sigma^2/2$ [44, Section 1.1]. The latter connection between random walks, Brownian motion, and the diffusion equation was noted by Einstein [29] in his most cited research paper. The corresponding connection between heavy tailed random walks, stable Lévy motion, and the FADE extends this powerful idea, see Sokolov and Klafter [61] for further discussion.

2.1 Fractional-Flux ADE (FF-ADE)

In a heterogeneous porous medium, at a large enough scale where the geological character of the medium changes with location, the material parameters v and D can depend on space. There are at least three variants of the FADE with space-dependent coefficients: 1) the fractional-flux ADE (FF-ADE), 2) the fractional-divergence ADE (FD-ADE), and 3) the fully fractional divergence ADE (FFD-ADE).

The FF-ADE model is derived from the classical conservation of mass (continuity) equation

$$\frac{\partial C}{\partial t} + \frac{\partial q}{\partial x} = 0, \tag{4}$$

where $q(x,t)$ is the flux, complemented with a fractional flux constitutive equation [51, 57]

$$q(x,t) = v(x)C - D(x)\frac{1+\beta}{2}\frac{\partial^{\alpha-1}C}{\partial x^{\alpha-1}} + D(x)\frac{1-\beta}{2}\frac{\partial^{\alpha-1}C}{\partial(-x)^{\alpha-1}}. \tag{5}$$

The first term in (5) is the *advective flux*, which models the average drift of contaminant particles, while the second and third terms are the *dispersive flux* that model large particle jumps in the positive and negative directions, respectively. Combining (4) and (5) yields the FF-ADE from Zhang et al. [67] and Huang et al. [33]:

$$\frac{\partial C}{\partial t} = -\frac{\partial}{\partial x}\left[v(x)C - D(x)\frac{1+\beta}{2}\frac{\partial^{\alpha-1}C}{\partial x^{\alpha-1}} + D(x)\frac{1-\beta}{2}\frac{\partial^{\alpha-1}C}{\partial(-x)^{\alpha-1}}\right]. \tag{6}$$

Setting $\beta = 1$ yields the FF-ADE given by Equation (4) in [68], while setting $v(x)$ and $D(x)$ constant yields (1).

2.2 Fractional-Divergence ADE (FD-ADE) and Fully Fractional Divergence ADE (FFD-ADE)

An alternative formulation replaces the divergence in the continuity equation (4) with a fractional divergence [43], yielding a fractional divergence-advection dispersion equation (FD-ADE)

$$\begin{aligned}\frac{\partial C}{\partial t} &= -\frac{\partial}{\partial x}[v(x)C] + \frac{1+\beta}{2}\frac{\partial^{\alpha-1}}{\partial x^{\alpha-1}}\left[D(x)\frac{\partial C}{\partial x}\right] \\ &\quad - \frac{1-\beta}{2}\frac{\partial^{\alpha-1}}{\partial(-x)^{\alpha-1}}\left[D(x)\frac{\partial C}{\partial x}\right].\end{aligned} \tag{7}$$

Setting $\beta = 1$ yields the FD-ADE given by Equation (11) in Zhang et al. [68]. By setting $v(x)$ and $D(x)$ constant in (7), we recover the *modified* FADE

$$\frac{\partial C}{\partial t} + v\frac{\partial C}{\partial x} = D\frac{1+\beta}{2}\frac{\partial^{\alpha-1}}{\partial x^{\alpha-1}}\left[\frac{\partial C}{\partial x}\right] - D\frac{1-\beta}{2}\frac{\partial^{\alpha-1}}{\partial(-x)^{\alpha-1}}\left[\frac{\partial C}{\partial x}\right], \tag{8}$$

proposed in Zhang et al. [66]. The modified FADE replaces the Riemann-Liouville fractional derivatives in the flux equation (5) with Caputo fractional derivatives. We will call the fractional derivatives on the right hand side of (8) *mixed Caputo* derivatives. These fractional derivatives, which lie in between the Riemann-Liouville and Caputo forms, have been used in various contexts, see for example Cushman and Ginn [21], Patie and Simon [52], and [43, Section 6]. On an infinite domain with sufficiently smooth concentration profiles that tend to zero at $\pm\infty$, both the FADE and the modified FADE are equivalent, because in that case the Riemann-Liouville and mixed Caputo derivatives are equal. On bounded domains, however, their behavior can be quite different. We will return to this issue in Subsection 6.2.

Finally, if we also fractionalize the advection term, we obtain the fully fractional divergence ADE (FFD-ADE):

$$\begin{aligned}\frac{\partial C}{\partial t} = -\frac{\partial^{\alpha-1}}{\partial x^{\alpha-1}}\left[v(x)C\right] + \frac{1+\beta}{2}\frac{\partial^{\alpha-1}}{\partial x^{\alpha-1}}\left[D(x)\frac{\partial C}{\partial x}\right] \\ -\frac{1-\beta}{2}\frac{\partial^{\alpha-1}}{\partial(-x)^{\alpha-1}}\left[D(x)\frac{\partial C}{\partial x}\right].\end{aligned} \tag{9}$$

All three versions of the FADE govern Markovian random walk processes, where the jump distribution depends on the current particle location [68]. The FF-ADE (6), FD-ADE (7), and FFD-ADE (9) can be discretized using an implicit Euler scheme, or alternatively a random walk particle tracking method [67]. The FF-ADE (6) and FD-ADE (7) exhibit similar plume behavior if $D(x)$ varies linearly with position x; however, for nonlinear $D(x)$ and small α near one, there is a significant difference between these two models. Finally, solutions to the the FFD-ADE (9) differ markedly from the FF-ADE and FD-ADE, with a much heavier leading tail. See Zhang et al. [68] for more details.

2.3 Fundamental Solutions

The solution to the FADE (1) on the real line with point-source initial condition $C(x,0) = \delta(x)$ for any $1 < \alpha \leq 2$ can be written in terms of a *stable* PDF $f(x;\alpha,\beta,\sigma,\delta)$ (e.g., see Samorodnitsky and Taqqu [55] or Meerschaert and Sikorskii [44, Proposition 5.8])

$$C(x,t) = f\left(x;\alpha,\beta,\left(Dt|\cos(\pi\alpha/2)|\right)^{1/\alpha}, vt\right). \tag{10}$$

For $\alpha = 2$, this solution reduces to a Gaussian. A brief derivation using Fourier transforms is included in Benson et al. [8] and [35]. Although the stable PDF

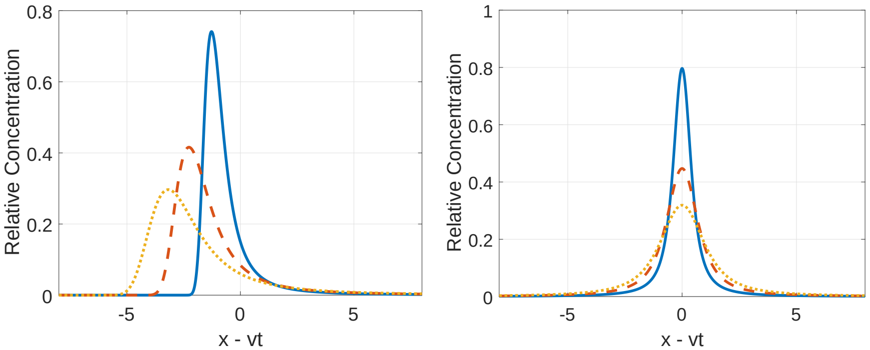

(a) $\beta = 1.0$ (skewed) (b) $\beta = 0$ (symmetric)

Fig. 2: Evolution of the point-source solution (10) at times $t = 1$ (solid), 2 (dashed), and 3 (dotted) relative to the plume center of mass. A stable index of $\alpha = 1.2$ and fractional dispersion coefficient of $D = 1$ are used. Panel a) shows a skewed plume with $\beta = 1$, while panel b) shows a symmetric ($\beta = 0$) plume.

with $1 < \alpha < 2$ cannot be written in closed form in terms of elementary functions, convenient computer codes are available to plot the stable PDF (e.g., see Nolan [50]) and these have been applied to the FADE [44, Chapter 5]. A MATLAB toolbox `FracFit`[1] to plot FADE solutions, and fit parameters to observed concentration data, is also available [34].

Figure 2 displays the evolution of the point-source solution (10) at times $t = 1$, 2, and 3 relative to the plume center of mass. A stable index of $\alpha = 1.2$ and fractional dispersion coefficient of $D = 1$ are used. Panel a) shows a skewed plume with $\beta = 1$, while panel b) shows a symmetric ($\beta = 0$) plume. In both panels, the solution has a nonlinear scaling rate proportional to $t^{1/\alpha}$, which grows faster than the classical Boltzmann rate $t^{1/2}$. That is, the point-source solution to the FADE exhibits super-diffusion. In addition, both figures exhibit heavy tails, which decay like inverse power laws with respect to x. For the skewed plume in panel a), the plume has a heavy tail to the right (downstream) of the plume center of mass $x = vt$, while in the symmetric case shown in panel b), the plume has heavy tails on both sides.

A second fundamental solution of interest to field and experimental hydrologists is a continuous injection solution. These solutions model continuous injection breakthrough curves (CBTCs) from laboratory experiments, such as transport of organic matter through porous media columns. These experiments

1 `https://github.com/jfk-inspire/FracFit-v-0.9` display strong anomalous transport characteristics, e.g., see Dietrich et al. [28] and McInnis et al. [38, 39].

At present, no closed form analytical solution for the FADE or the FD-ADE using a continuous injection on the half-axis exists; however, an analytical approximation following what is done for the classical ADE ($\alpha = 2$) in Danckwerts [22] may be derived as follows. Consider the modified FADE (8) on $-\infty < x < \infty$ subject to initial condition $C_0(x, 0) = C_0$ for $x < 0$ and $C_0(x, 0) = 0$ for $x \geq 0$. Using the FADE pulse initial condition solution (10) , the continuous injection solution is approximated by

$$C(x,t) = \int_{-\infty}^{\infty} C_0(x') f\left(x - x'; \alpha, \beta, (Dt|\cos(\pi\alpha/2)|)^{1/\alpha}, vt\right) dx'. \tag{11}$$

Evaluating the integral in (11)) yields

$$C(x,t) = C_0\left[1 - F\left(x; \alpha, \beta, (Dt|\cos(\pi\alpha/2)|)^{1/\alpha}, vt\right)\right], \tag{12}$$

where $F(z; \alpha, \beta, \sigma, \delta)$ denotes the cumulative distribution function (CDF) for a stable random variable.

To verify this approximation, we compare it to a complete numerical solution from Zhang et al. [66]. A prescribed concentration boundary condition was imposed at the inlet $C(0, t) = C_0 H(t)$ and a free drainage boundary condition was imposed at $x = L = 200$. The parameters used in both simulations are $D = 2.5$, $v = 10.0$, $\alpha = 1.6$, which are identical to those used in Fig. 3a of [66]. Agreement between (12) and the numerical solution is very good, indicating that (12) is a good approximation for continuous injection. For the case $\beta = 1$ shown in panel a), we can see a heavier leading tail, while for the case $\beta = -1$ plotted in panel b), we can observe a heavy trailing tail.

3 Multidimensional Fractional Advection-Dispersion Equation

A multi-dimensional FADE was proposed in [40]

$$\frac{\partial C}{\partial t} + \mathbf{v} \cdot \nabla C(\mathbf{x}, t) = D\nabla_M^\alpha C(\mathbf{x}, t), \tag{13}$$

where $\mathbf{v}$ [L/T] is the d-dimensional average plume velocity and ∇_M^α is a vector fractional derivative [43] defined via an inverse spatial Fourier transform

$$\nabla_M^\alpha C(\mathbf{x}, t) = \mathcal{F}^{-1}\left[\int_{\|\boldsymbol{\theta}\|=1} (i\mathbf{k} \cdot \boldsymbol{\theta})^\alpha \hat{C}(\mathbf{k}, t) M(d\boldsymbol{\theta})\right], \tag{14}$$

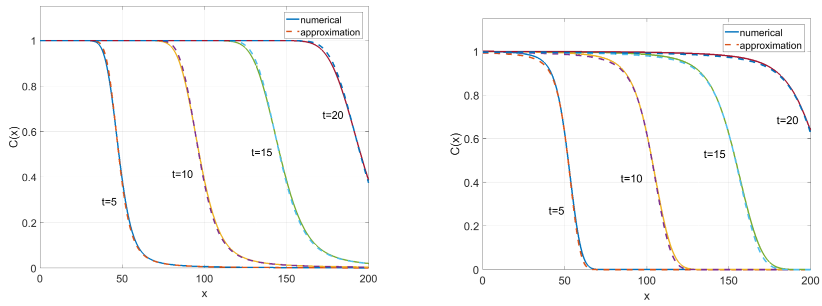

(a) $\beta = 1.0$ (b) $\beta = -1.0$

Fig. 3: Comparison of the analytical approximation given by Eq. (12) and a semi-implicit discretization of the modified FADE (8). The unitless parameters for the two simulation are $C_0 = 1$, $\alpha = 1.6$, $v = 10$, $D = 2.5$. The left panel is positively-skewed ($\beta = 1.0$), while the right panel is negatively-skewed ($\beta = -1.0$).

where $\boldsymbol{\theta}$ is an d-dimensional unit vector, $\mathbf{k}$ is a wave-vector, $\hat{C}(\mathbf{k}, t) = \mathcal{F}[C(\mathbf{x}, t)] = \int e^{-i\mathbf{k}\cdot\mathbf{x}} C(\mathbf{x}, t)\, d\mathbf{x}$ is the spatial Fourier transform of concentration, and $M(d\boldsymbol{\theta})$ is a mixing measure defined over the unit sphere in d-dimensions. If $\alpha = 2$, (13) reduces to the traditional vector ADE

$$\frac{\partial C}{\partial t} + \mathbf{v} \cdot \nabla C(\mathbf{x}, t) = \nabla \cdot A \nabla C(\mathbf{x}, t)$$

where the 2-tensor

$$A = D \int \boldsymbol{\theta}\boldsymbol{\theta}^T M(d\boldsymbol{\theta})$$

is the dispersion tensor using the outer product [44, Section 6.5]. For a general mixing measure with $1 < \alpha < 2$, fundamental solutions to (13) cannot be expressed in closed form. We will consider two special cases, in which case we can write the fundamental solutions as products of stable PDFs. If jumps only occur along the standard coordinate vectors $\mathbf{e}_j : j = 1, 2, \ldots, d$ with probabilities $M\{\mathbf{e}_j\} = p/d$ and $M\{-\mathbf{e}_j\} = q/d$, then the fractional directional derivative (14) is evaluated as

$$\nabla^{\alpha}_{M} C(\mathbf{x}, t) = \frac{p}{d} \sum_{j=1}^{d} \frac{\partial^{\alpha}}{\partial x_j^{\alpha}} C(\mathbf{x}, t) + \frac{q}{d} \sum_{j=1}^{d} \frac{\partial^{\alpha}}{\partial(-x_j)^{\alpha}} C(\mathbf{x}, t). \tag{15}$$

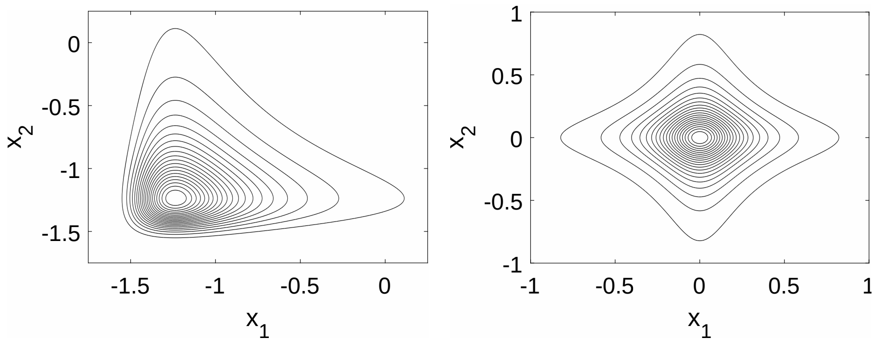

(a) $\beta = 1.0$ (skewed) (b) $\beta = 0$ (symmetric)

Fig. 4: Level sets of the point-source solution to the multi-dimensional FADE ($d = 2$) at time $t = 1$ relative to the plume center of mass. A stable index of $\alpha = 1.1$ and fractional dispersion coefficient of $D_0 = 1$ are used. Panel a) shows contours of a skewed plume with $\beta = 1$, while panel b) shows contours of a symmetric ($\beta = 0$) plume.

Letting $D_0 = D/d$ and $\beta = p - q$ yields a vector fractional diffusion equation

$$\frac{\partial}{\partial t} C(\mathbf{x}, t) + \mathbf{v} \cdot \nabla C(\mathbf{x}, t) = D_0 \frac{1+\beta}{2} \sum_{j=1}^{d} \frac{\partial^\alpha}{\partial x_j^\alpha} C(\mathbf{x}, t) + D_0 \frac{1-\beta}{2} \sum_{j=1}^{d} \frac{\partial^\alpha}{\partial (-x_j)^\alpha} C(\mathbf{x}, t). \quad (16)$$

Assuming a velocity $\mathbf{v} = \sum_{j=1}^{d} v_j \mathbf{e}_j$, the point source solution to (16) with $C(\mathbf{x}, 0) = \delta(\mathbf{x})$ may be computed via a Fourier transform, yielding

$$C(\mathbf{x}, t) = \prod_{j=1}^{d} f\left(x_j; \alpha, \beta, (D_0 t |\cos(\pi\alpha/2)|)^{1/\alpha}, v_j t\right). \quad (17)$$

Figure 4 shows level sets of (17) for $d = 2$ dimensions at time $t = 1$ relative to the plume center of mass. A stable index of $\alpha = 1.1$ and fractional dispersion coefficient of $D_0 = 1$ are used. Panel a) shows contours of a skewed plume with $\beta = 1$, while panel b) shows contours of a symmetric ($\beta = 0$) plume. Note that the contours are anisotropic in both cases, including panel b) with symmetric jumps ($\beta = 0$). Except for $\alpha = 2$, the plume spreads in an asymmetric fashion, thus providing a good model for anisotropic media.

Finally, consider the case where $M(d\boldsymbol{\theta})$ is uniform over the $(d-1)$-dimensional sphere. Using [44, Example 6.24], (14) is evaluated as the (symmetric) fractional Laplacian, yielding

$$\frac{\partial}{\partial t}C(\mathbf{x},t) + \mathbf{v}\cdot\nabla C(\mathbf{x},t) = c_\alpha D\Delta^{\alpha/2}C(\mathbf{x},t), \tag{18}$$

where $\Delta^{\alpha/2}C(\mathbf{x},t)$ has Fourier transform $-|\mathbf{k}|^\alpha\hat{C}(\mathbf{k},t)$ and c_α is a coefficient that only depends on the order α. The fundamental solution may be written as a subordinated normal PDF [44, Example 6.5], yielding a *symmetric* level set. Further extensions of the FADE in multiple dimensions are developed in Schumer et al. [59], see also [41,68] and [44, Chapter 6]. This *operator scaling* FADE allows a different order of the space-fractional derivative in each coordinate.

4 Time-Fractional Models

Unlike the space FADE, which models long particle jumps, the time-fractional FADE models long waiting times between jumps, by replacing the first-order time-derivative in the ADE with a time-fractional derivative. In this section, we summarize two widely used time-fractional PDEs: the time-fractional FADE and the fractional mobile-immobile equation (FMIM). In Subsection 6.1, we will see how the space FADE and time FADE are related via duality.

4.1 Time-Fractional FADE

The time-fractional advection dispersion equation from Zaslavsky [63] or Liu et al. [36] is given by

$$\left(\frac{\partial}{\partial t}\right)^\gamma C = -v\frac{\partial C}{\partial x} + D\frac{\partial^2 C}{\partial x^2}, \tag{19}$$

where the first term in (19) is a Caputo derivative with order $0<\gamma<1$ on the half-axis. In the case of $\gamma = 1$, (19) reduces to the classical ADE. In contrast to the spatial FADE (1), the units of the velocity parameter v are $\mathrm{L}/\mathrm{T}^\gamma$ and the units of the dispersion coefficient are $\mathrm{L}^2/\mathrm{T}^\gamma$.

This time-fractional equation governs the scaling limit of a continuous time random walk (CTRW). For simplicity, suppose that $v = 0$. Assume as in Section 2 that $S_n = X_1 + \cdots + X_n$ is a random walk of particle jumps. Now suppose that a random waiting time W_n occurs before the nth jump. The random walk $T_n = W_1+\cdots+W_n$ gives the time of the nth jump, $N(t) = \max\{n \ge 0 : T_n \le t\}$ is the number of jumps by time $t \ge 0$, and the CTRW $S_{N(t)}$ is the location of a randomly selected particle at time $t \ge 0$. If the waiting times are heavy tailed with $\mathbb{P}[W_n > t] = At^{-\gamma}$ for some $A > 0$ and $0 < \gamma < 1$, then

$$n^{-1/\gamma} \sum_{j=1}^{[nt]} W_j = n^{-1/\gamma} T_{[nt]} \Rightarrow D_t, \tag{20}$$

another stable Lévy motion called a stable subordinator. The counting process $n^{-\gamma} N(nt) \Rightarrow E(t)$, where $E(t) = \inf\{u > 0 : D_u > t\}$ is called the inverse stable subordinator, and a continuous mapping argument yields the CTRW limit $Z_{E(t)}$ [44, Section 4.4]. The PDF $C(x,t)$ of the CTRW limit is the point source solution to the time-fractional dispersion equation (19) [42]. From a hydrological point of view, the waiting times model resting periods between particle movements.

Closed-form solutions to (19) are constructed via subordination. Starting with a solution $C_{\text{ADE}}(x,t)$ to the ADE (19) with $\gamma = 1$, the time variable is randomized by the inverse stable subordinator (e.g., see Meerschaert and Straka [45]). For a pulse initial condition $C(x,0) = \delta(x)$ on the real axis, this subordination integral is written as [44, Equation (4.39)]

$$C(x,t) = \int_0^\infty h_\gamma(u,t) \frac{1}{\sqrt{4\pi D u}} \exp\left(-\frac{(x - vu)^2}{4Du}\right) du, \tag{21}$$

where $h_\gamma(u,t)$ is the pdf of the inverse γ-stable subordinator $E(t)$. The density $h_\gamma(u,t)$ may be written in terms of a stable density [44, Equation (4.47)], and evaluated using available codes (e.g., Nolan [50] or [34]).

4.2 Fractional Mobile Immobile Equation

The fractional mobile-immobile (FMIM) model from Schumer et al. [58] generalizes the classical mobile-immobile (MIM) model (e.g., see Coats and Smith. [18]), which partitions the concentration into mobile $C_m(x,t)$ and immobile $C_{im}(x,t)$ phases. All MIM models equate the divergence of the total (advective and dispersive) flux to a weighted sum of the time rate of change of each phase. The rate of change from the immobile to the mobile phase is expressed as a convolution with a memory function $f(t)$. In particular, the FMIM model [58] uses a power law memory function $f(t) = t^{-\gamma}/\Gamma(1-\gamma)$ with $0 < \gamma < 1$.

A CTRW model for the FMIM, that segregates mobile from immobile particles, was developed by Benson and Meerschaert [10]. It models the long waiting times experienced by solute particles in the immobile phase by a power law, exactly as for the time-FADE. The memory function is explicitly computed in terms of the CTRW model. Power law waiting times have been observed in river transport studies by Haggerty et al. [32] and Schmadel et al. [56].

The FMIM equation with Fickian flux for mobile concentration is given by Schumer et al. [58] as

$$\frac{\partial C_m}{\partial t} + \beta_c \frac{\partial^\gamma C_m}{\partial t^\gamma} = -v\frac{\partial C_m}{\partial x} + D\frac{\partial^2 C_m}{\partial x^2}, \tag{22}$$

where the second term in (22) is a Riemann-Liouville derivative on the half-axis, β_c [$\mathrm{T}^{\gamma-1}$] is the capacity coefficient, defined as the ratio of the porosity in the immobile phase to that of the mobile phase (see Haggerty and Gorelick [30]), D [L^2/T] is the dispersion coefficient, and v [L/T] is the average velocity. This FMIM is similar to an earlier model proposed in Carrera et al. [15] and to a truncated power-law model proposed in Haggerty et al. [31].

Like the time-FADE, solutions to (22) may be expressed via a subordination integral [58, Equation (21)]

$$C_m(x,t) = \int_0^t g_\gamma\left(t-u, \beta_c u\right) \frac{1}{\sqrt{4\pi D u}} \exp\left(-\frac{(x-vu)^2}{4Du}\right) du, \tag{23}$$

where $g_\gamma(t,u)$ is the density of the γ-stable subordinator D_u, with Laplace transform $\tilde{g}(s,u) = e^{-us^\gamma}$. A calculation [58] shows that $C_m(x,t)$ falls off like $t^{-\gamma-1}$ at late time.

5 Parameter Estimation and Source Identification

Application of the FADE to observed field or laboratory data often requires solving an inverse problem. In this section, we briefly discuss two such inverse problems: source identification and parameter identification.

5.1 Source Identification

In groundwater hydrology, source identification determines the source location, release history, and/or strength of a contaminant source given one or more measurements. One approach is to solve the forward equation multiple times to identify the source. While straightforward, this method is computationally expensive. Alternatively, one may derive a *backward equation* whose solution is a PDF for the source location/time. This backward equation only needs to be solved once, and is hence computationally more efficient.

A backward model for the classical ADE was derived in Neupauer and Wilson [49] using an adjoint-based approach. This method was extended to the

FADE (specifically, the FD-ADE) in Zhang et al. [71] and later to bounded domains in Zhang et al. [72]. Since the primary application is groundwater flows, we consider a special case of the FD-ADE (7) with only positive jumps ($\beta = 1$) and source and sink terms given by [71, Equation 1 with effective porosity $\theta = 1$]

$$\frac{\partial}{\partial t}C = -\frac{\partial}{\partial x}\left[v(x)C\right] + \frac{\partial}{\partial x}\left[D(x)\frac{\partial^{\alpha-1}C}{\partial x^{\alpha-1}}\right] + q_i C_i - q_0 C, \tag{24}$$

where the mean velocity v and dispersion coefficient D may vary with x (heterogeneous), q_i is the source inflow rate, q_0 is the sink outflow rate, and C_i is the inflow concentration. Letting $A(x,t)$ be the adjoint state, the backward FADE is given by [71, Equation 10 with $\theta = 1$]

$$\frac{\partial}{\partial t}A = \frac{\partial}{\partial x}\left[v(x)A\right] + \frac{\partial^{\alpha-1}}{\partial(-x)^{\alpha-1}}\left[D(x)\frac{\partial A}{\partial(-x)}\right] - q_i A + \delta(x - x_d)\delta(\tau), \tag{25}$$

where x_d is the detection location, T is the detection time, and $\tau = T - t$ is the “backward time”. Given an observed contaminant at location x_d at backward time $\tau = 0$ assuming no other source or sink, the backward location PDF $f_x(x;\tau)$ satisfies (25) with $q_i = 0$. If both v and D are assumed constant, then (25) has an analytical solution specified by (10):

$$f_x(x;\tau) = f\left(x - x_d; \alpha, -1, \left(D\tau|\cos(\pi\alpha/2)|\right)^{1/\alpha}, v\tau\right). \tag{26}$$

Figure 5 evaluates the PDF (26) using MADE-2 concentration data [12] for day a) 132, b) 224, and c) 328 using $\alpha = 1.1$, $v = 0.12$ m/day, and $D = 0.14$ m$^\alpha$/day. The vertical solid bar shows the actual release location, while the long and short dashed lines show the 75th and 25th percentiles of the displayed PDF. Although the predicted source location does not coincide with the median, the predicted source location does lie between the 25th and 75th percentiles. The variability in this estimation motivates further study, such as including a scale dependent dispersion coefficient and the effects of a finite boundary [72].

5.2 Parameter Estimation

A statistically optimal parameter estimation method based on the weighted nonlinear least squares (WNLS) approach is described in Chakraborty et al. [16]. This method is applicable to both snapshot data $x \mapsto C(x,t)$ with time t fixed and breakthrough curve (BTC) data $t \mapsto C(x,t)$ with position x fixed. Using a particle-tracking approach, [16] demonstrated that concentration variance is proportional to concentration (heteroscedasticity). As a result, weighted nonlinear

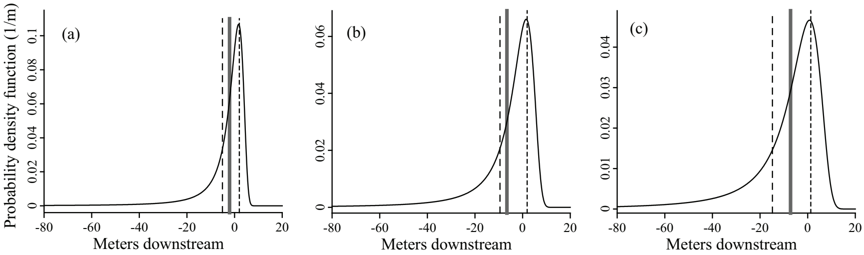

Fig. 5: PDF of contaminant release location predicted by the backward FADE using MADE-2 concentration data for day a) 132, b) 224, and c) 328 using $\alpha = 1.1$, $v = 0.12$ m/day, and $D = 0.14$ m$^{\alpha}$/day. The vertical solid bar shows the actual release location, while the long and short dashed lines show the 75th and 25th percentiles of the displayed PDF. Reprinted from [71].

regression is used where the weights are proportional to the reciprocal of measured concentration, thereby assigning a greater weight to lower concentration values. This WNLS approach is important for capturing anomalous transport characteristics (e.g., heavy leading or trailing tails). This estimation procedure was adapted to time-fractional, tempered time-fractional models (e.g., see [48]), and continuous injection data in [34].

To illustrate the WNLS approach, assume we have N measurements of a BTC $C_i = C(x, t_i)$ at times $t_i, 1 \le i \le N$, and we wish to fit the parameters $\Theta = (\alpha, \beta, v, D)$ of the FADE to observed data by minimizing the weighted mean square error (WMSE) function

$$E(\Theta) = \frac{1}{N} \sum_{i=1}^{N} w_i \left(C_i - C(x, t_i)\right)^2, \tag{27}$$

where $C(x, t)$ is the modeled concentration (e.g., (10) for the space FADE) and the weights are given by $w_i = 1/C_i$. Either local optimization using a reasonable guess or global optimization (e.g., genetic algorithm) may be used to minimize (27) to find the optimal parameters Θ. We fit both the spatial FADE model (1) and the fractional mobile-immobile (FMIM) model, (22) and compare the results, using the `FracFit` package.

The first dataset is from a fluorescein dye tracer test conducted in the Red Cedar River (Michigan, USA) by Phanikumar et al. [53]. BTCs were measured at locations $x = 1.4$ km, 3.1 km, and 5.08 km downstream of the tracer source. The data was fit to the FADE (1) in previous work [16]. We replicated that fit at these three locations and also fit the FMIM model (22). The model fits and data are shown in panel a) of Figure 6 for location $x = 3.1$ km. The FMIM parameters are $\gamma = 0.96$, $v = .145$ km/min, $\beta_c = 3.87$ min$^{-.04}$, and $D = .0012$

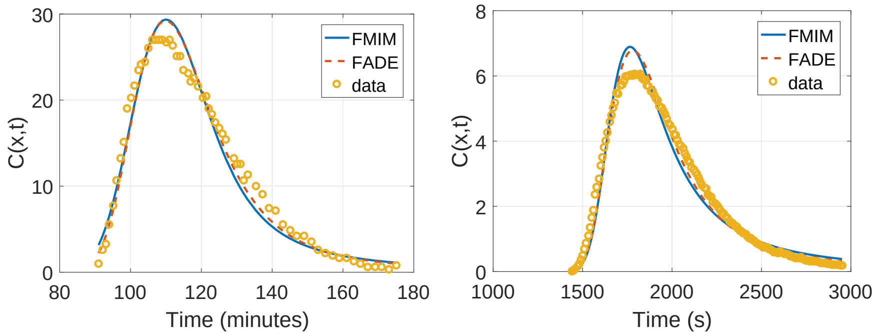

(a) Red Cedar river (b) Selke river

Fig. 6: BTCs for the Red Cedar river at $x = 3.1$ km (panel a) and the Selke river at $x = 667$ m (panel b). The FADE (1) and time-fractional model (22) are fit using the `FracFit` toolbox. Parameters are given in the text.

km^2/min. The FADE parameters are $\alpha = 1.56$, $\beta = -1$, $v = .0259$ km/min, and $D = .0013$ km$^{1.56}$/min. It is apparent that both models fit the data reasonably well.

The second dataset is a similar dye tracer test conducted in the Selke River (Germany) by Schmadel et al. [56]. Eight tracer injections were released and measured at seven downstream locations. We fit data from injection 7 at site 4, located 667 m downstream. The optimal fits and data are shown in panel b) of Figure 6. The FMIM parameters are $\gamma = 0.906$, $v = 0.8549$ m/s, $\beta_c = 0.844$ s$^{-0.094}$, and $D = 0.3204$ m^2/s. The FADE parameters are $\alpha = 1.33$, $\beta = -1$, $v = 0.313$ m/s, and $D = 0.223$ m$^{1.56}$/s. Again, both models match the data reasonably well. These parameter fits suggest that there could be a relationship between time-fractional models and the space-FADE, which is discussed in the next section.

6 Current and Future Research

6.1 Space-Time Duality

As the parameter fits in Figure 6 illustrate, applications of the FADE to river flow hydrology employ a negatively skewed space-fractional derivative ($\beta = -1$), which models long upstream jumps in the random walk model outlined in Section 2. Deng et al. [27] suggest that this negatively skewed space-fractional derivative is capturing a “wide spectrum of dead zones” in the velocity field. The time-FADE models particle retention using a time-fractional derivative, which captures long resting periods between particle movements in the CTRW model discussed in Section 4. Zhang et al. [69] recommend the time-FADE (19) instead of the negatively skewed FADE (1) to model contaminant transport in rivers, because it does not seem physical for particles to make long upstream jumps. However, it is important to note that these jumps are moving upstream *relative to the center of mass*. In the space-FADE model, a particle moves downstream and then jumps back upstream. In the time-FADE model, the particle remains upstream while the bulk of the plume moves downstream. Either way, the particle ends up behind the plume center of mass.

This controversy between the space-FADE and the time-FADE for river flows was resolved in [35] by establishing a mathematical equivalence between the negatively skewed space-FADE and the time-FADE. This duality principle, which was applied to the space-fractional diffusion equation in Baeumer et al. [5], can be illustrated by considering the point source solution $C_0(x,t)$ to the negatively skewed FADE (1) with $\beta=-1$, $v=0$ and $D=1$:

$$\frac{\partial C_0}{\partial t}=\frac{\partial^\alpha C_0}{\partial(-x)^\alpha}. \tag{28}$$

Apply a Fourier transform with respect to both x and t, yielding

$$[(i\omega)-(-ik)^\alpha]\hat{C}_0(k,\omega)=0, \tag{29}$$

where k is the the wavenumber and ω is the angular frequency. This *dispersion relationship* is equivalent to $(i\omega)^\gamma=(-ik)$ where $\gamma=1/\alpha$. Substituting back into (29) and inverting the FT leads to the *dual equation*

$$\frac{\partial^\gamma C_0}{\partial t^\gamma}=-\frac{\partial C_0}{\partial x} \tag{30}$$

since $\partial/\partial(-x)=-\partial/\partial x$. Note that (30) is a special case of the time FADE (19) with v =1 and $D=0$ using a Caputo derivative. In the case $\alpha=2$ ($\gamma=1/2$), this space-time duality for the traditional diffusion equation was observed by Heaviside in 1871, perhaps the first real application of the fractional calculus. A rigorous derivation of space-time duality is laid out in [35], including the FADE (1) with any skewness. If the advection term in (1) is retained, it is shown in [35] that the dual time-fractional PDE involves the *fractional material derivative* from Sokolov and Metzler [60].

6.2 FADE in Bounded Domains

Most problems in hydrology and fluid dynamics occur on bounded domains, such as contaminant transport in column experiments [38,39]. Application of the FADE on a bounded domain is a challenging problem, since the boundary condition may itself be nonlocal. Most available numerical schemes assume Dirichlet boundary conditions (BCs), including finite difference methods [46, 47, 54] and spectral methods [37, 64]; however, many problems involving the FADE in bounded domains require either mass conservation or a specification of flux. Considerable effort has been spent on developing mass-preserving, *reflecting* BCs for space fractional diffusion equations [3,4,23]. In particular, Baeumer et al. [3] proposed explicit Euler schemes for the one dimensional space-FADE using either a positive RL derivative or a mixed Caputo derivative. They show that the appropriate mass-preserving schemes involve a *fractional* boundary condition. The same fractional BCs were also applied to the (forward) FADE in Zhang et al. [70] and to the backward FADE in Zhang et al. [72].

As a simple example, consider the FADE model (1) on the unit interval $[0, 1]$ with $v(x) = 0$, $D(x) = 1$ and $\beta = 1$. Assume some initial mass $M_0 = \int_0^1 C(x,t)\,dx$ is conserved for all time t. Integrating the mass conservation equation (4) with respect to x and applying the fundamental theorem of calculus yields

$$\begin{aligned}\frac{\partial M_0}{\partial t} &= \int_0^1 \frac{\partial}{\partial t} C(x,t)\,dx \\ &= -\int_0^1 \frac{\partial}{\partial x} q(x,t)\,dx \\ &= q(0,t) - q(1,t).\end{aligned}$$

If the flux $q(0, t)$ and $q(1, t)$ at both endpoints is identically zero, then mass is conserved. From (5), the zero flux BC is

$$\left.\frac{\partial^{\alpha-1} C}{\partial x^{\alpha-1}}\right|_{x=0} = \left.\frac{\partial^{\alpha-1} C}{\partial x^{\alpha-1}}\right|_{x=1} = 0. \tag{31}$$

Figure 7 shows a numerical solutions using the explicit Euler method outlined in Baeumer et. al. [3] of a) the FADE (1) with Riemann-Liouville reflecting boundary conditions (31) and b) the FADE with Caputo flux (8) with Caputo reflecting boundary conditions. As t increases, the solution in Figure 7(a) converges to the steady-state solution $C_\infty(x) = M_0(\alpha-1)x^{\alpha-2}$, which is singular at $x = 0$. Figure 7(b) shows numerical solutions of the modified FADE (8) with zero flux BCs. These BCs are the same as (31), except that the Riemann-Liouville

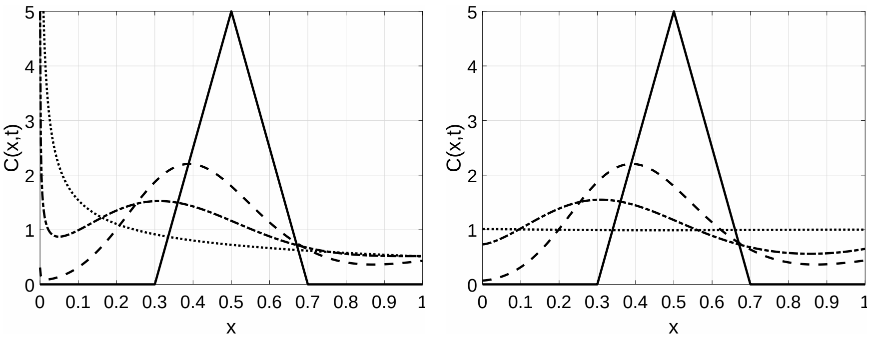

(a) Riemann-Liouville reflecting BC

(b) Caputo reflecting BC

Fig. 7: Numerical solution of a) the FADE (1) with Riemann-Liouville reflecting boundary conditions (31) and b) the FADE with Caputo flux (8) with Caputo reflecting boundary conditions. Both panels use parameters $\alpha = 1.5$, $v = 0$, $\beta = 1$, and $D = 1$ on $0 \leq x \leq 1$ at time $t = 0$ (solid line), $t = 0.05$ (dashed), $t = 0.1$ (dash dot), $t = 0.5$ (dotted).

fractional derivatives are replaced by Caputo derivatives. Since the Caputo fractional derivative of a constant is zero, the steady state solution is a constant $C_\infty(x) = M_0$. Consideration of the steady state solution is one useful method for selecting the appropriate FADE model on a bounded domain.

7 Summary

The space FADE (1) models a wide range of observed anomalous dispersion using a fractional RL derivative in space. This RL derivative is a nonlocal operator and models large jumps of solute particles in heterogeneous media. The fundamental solutions to the space FADE in 1D exhibit both heavy tails and skewness, which are observed in many tracer tests. The space FADE has been extended to media with space-dependent material parameters and multiple dimensions. The time FADE and fractional mobile immobile (FMIM) models, which utilize time-fractional derivatives to model long-waiting times (retention), are also used to model anomalous dispersion. A connection between long upstream particle jumps and long waiting times is established using space-time duality, which provides an equivalence between the negatively-skewed space FADE and the time FADE. Finally, the FADE in bounded domains with nonlocal, reflecting boundary conditions is discussed.

Acknowledgment: JFK was partially supported by ARO MURI grant W911NF-15-1-0562 and NSF grant EAR-1344280. MMM was partially supported by ARO MURI grant W911NF-15-1-0562 and NSF grants DMS-1462156 and EAR-1344280. The authors thank Noah Schmadel and Adam S. Ward (Department of Environmental Engineering, Indiana University) for providing the Selke River data and Yong Zhang (Department of Geological Sciences, University of Alabama) for Figure 5.

References

[1] E. J. Anderson and M. S. Phanikumar. Surface storage dynamics in large rivers: Comparing three-dimensional particle transport, one-dimensional fractional derivative, and multirate transient storage models. *Water Resources Research*, 47(9):W09511, 2011.

[2] A. Aubeneau, B. Hanrahan, D. Bolster, and J. Tank. Substrate size and heterogeneity control anomalous transport in small streams. *Geophysical Research Letters*, 41:8335–8341, 2014.

[3] B. Baeumer, M. Kovács, M. M. Meerschaert, and H. Sankaranarayanan. Boundary conditions for fractional diffusion. *Journal of Computational and Applied Mathematics*, 336:408-424, 2018.

[4] B. Baeumer, M. Kovács, and H. Sankaranarayanan. Fractional partial differential equations with boundary conditions. *Journal of Differential Equations*, 264:1377–1410, 2018.

[5] B. Baeumer, M. M. Meerschaert, and E. Nane. Space–time duality for fractional diffusion. *Journal of Applied Probability*, 46:1100–1115, 2009.

[6] J. Bear. *Dynamics of Fluids in Porous Media*, Elsevier, New York, 1972.

[7] D. A. Benson, S. W. Wheatcraft, and M. M. Meerschaert. Application of a fractional advection-dispersion equation. *Water Resources Research*, 36(6):1403–1412, 2000.

[8] D. A. Benson, S. W. Wheatcraft, and M. M. Meerschaert. The fractional-order governing equation of Lévy motion. *Water Resources Research*, 36(6):1413–1423, 2000.

[9] D. M. Benson, R. Schumer, M. M. Meerschaert, and S. W. Wheatcraft. Fractional dispersion, Lévy motion, and the MADE tracer tests. *Transport in Porous Media*, 42:211–240, 2001.

[10] D. A. Benson and M. M. Meerschaert. A simple and efficient random walk solution of multi-rate mobile/immobile mass transport equations. *Advances in Water Resources*, 32:532–539, 2009.

[11] B. Berkowitz and H. Scher. Anomalous transport in random fracture networks. *Physical Review Letters*, 79:4038, 1997.

[12] J. M. Boggs, S. C. Young, L. M. Beard, L. W. Gelhar, K. R. Rehfeldt, and E. E. Adams. Field study of dispersion in a heterogeneous aquifer: 1. overview and site description. *Water Resources Research*, 28(12):3281–3291, 1992.

[13] D. Bolster, D. A. Benson, T. Le Borgne, and M. Dentz. Anomalous mixing and reaction induced by superdiffusive nonlocal transport. *Physical Review E*, 82(2):021119, 2010.

[14] D. Bolster, D. A. Benson, M. M. Meerschaert, and B. Baeumer. Mixing-driven equilibrium reactions in multidimensional fractional advection–dispersion systems. *Physica A: Statistical Mechanics and its Applications*, 392(10):2513–2525, 2013.

[15] J. Carrera, X. Sánchez-Vila, I. Benet, A. Medina, G. Galarza, and J. Guimerà. On matrix diffusion: Formulations, solution methods and qualitative effects. *Hydrogeology Journal*, 6(1):178–190, 1998.

[16] P. Chakraborty, M. M. Meerschaert, and C. Y. Lim. Parameter estimation for fractional transport: A particle-tracking approach. *Water Resources Research*, 45(10):W10415, 2009.

[17] D. D. Clarke, M. M. Meerschaert, and S. W. Wheatcraft. Fractal travel time estimates for dispersive contaminants. *Groundwater*, 43(3):401–407, 2005.

[18] K. Coats and B. Smith. Dead-end pore volume and dispersion in porous media. *Society of Petroleum Engineers Journal*, 4(1):73–84, 1964.

[19] A. Cortis and B. Berkowitz. Anomalous transport in "classical" soil and sand columns. *Soil Science Society of America Journal.* 68(5):1539–1548, 2004.

[20] J. H. Cushman and T. Ginn. Nonlocal dispersion in media with continuously evolving scales of heterogeneity. *Transport in Porous Media*, 13(1):123–138, 1993.

[21] J. H. Cushman and T. R. Ginn. Fractional advection-dispersion equation: a classical mass balance with convolution-fickian flux. *Water Resources Research*, 36(12):3763–3766, 2000.

[22] P. Danckwerts. Continuous flow systems: Distribution of residence times. *Chemical Engineering Science*, 2(1):1–13, 1953.

[23] D. del-Castillo-Negrete. Fractional diffusion models of nonlocal transport. *Physics of Plasmas*, 13: 082308, 2006.

[24] O. Defterli, M. D'Elia, Q. Du, M. Gunzburger, R. Lehoucq, and M. M. Meerschaert. Fractional diffusion on bounded domains. *Fractional Calculus and Applied Analysis*, 18(2): 342–360, 2015.

[25] Z. Deng, L. Bengtsson, and V. P. Singh. Parameter estimation for fractional dispersion model for rivers. *Environmental Fluid Mechanics*, 6(5):451–475, 2006.

[26] Z.-Q. Deng, J. L. De Lima, M. I. P. de Lima, and V. P. Singh. A fractional dispersion model for overland solute transport. *Water Resources Research*, 42(3): W03416, 2006.

[27] Z.-Q. Deng, V. P. Singh, and L. Bengtsson. Numerical solution of fractional advection-dispersion equation. *Journal of Hydraulic Engineering*, 130(5):422–431, 2004.

[28] L. Dietrich, D. McInnis, D. Bolster, and P. Maurice. Effect of polydispersity on natural organic matter transport. *Water Research*, 47:2231–2240, 2013.

[29] A. Einstein. On the movement of small particles suspended in a stationary liquid demanded by the molecular kinetic theory of heat. *Annals of Physics* 17:549–560, 1905.

[30] R. Haggerty and S. M. Gorelick. Multiple-rate mass transfer for modeling diffusion and surface reactions in media with pore-scale heterogeneity. *Water Resources Research*, 31(10):2383–2400, 1995.

[31] R. Haggerty, S. A. McKenna, and L. C. Meigs. On the late-time behavior of tracer test breakthrough curves. *Water Resources Research*, 36(12):3467–3479, 2000.

[32] R. Haggerty, S. M. Wondzell, and M. A. Johnson. Power-law residence time distribution in the hyporheic zone of a 2nd-order mountain stream. *Geophysical Research Letters*, 29(13):18–1, 2002.

[33] G. Huang, Q. Huang, and H. Zhan. Evidence of one-dimensional scale-dependent fractional advection–dispersion. *Journal of Contaminant Hydrology*, 85(1):53–71, 2006.

[34] J. F. Kelly, D. Bolster, M. M. Meerschaert, J. A. Drummond, and A. I. Packman. FracFit: A robust parameter estimation tool for fractional calculus models. *Water Resources Research*, 53(3):2559–2567, 2017.

[35] J. F. Kelly and M. M. Meerschaert. Space-time duality for the fractional advection dispersion equation. *Water Resources Research*, 53(4):3464–3475, 2017.

[36] F. Liu, V. V. Anh, I. Turner, and P. Zhuang. Time fractional advection-dispersion equation. *Journal of Applied Mathematics and Computing*, 13(1):233–245, 2003.

[37] Z. Mao, S. Chen, and J. Shen. Efficient and accurate spectral method using generalized Jacobi functions for solving riesz fractional differential equations. *Applied Numerical Mathematics*, 106:165–181, 2016.

[38] D. P. McInnis, D. Bolster, and P. A. Maurice. Natural organic matter

transport modeling with a continuous time random walk approach. *Environmental Engineering Science*, 31(2):98–106, 2014.

[39] D. P. McInnis, D. Bolster, and P. A. Maurice. Mobility of dissolved organic matter from the Suwannee river (Georgia, USA) in sand-packed columns. *Environmental Engineering Science*, 32(1):4–13, 2015.

[40] M. M. Meerschaert, D. A. Benson, and B. Baeumer. Multidimensional advection and fractional dispersion. *Physical Review E*, 59(5):5026, 1999.

[41] M. M. Meerschaert, D. A. Benson and B. Baeumer. Operator Lévy motion and multiscaling anomalous diffusion. *Physical Review E*, 63:021112–021117, 2001.

[42] M. M. Meerschaert, D. A. Benson, H.-P. Scheffler, and B. Baeumer. Stochastic solution of space-time fractional diffusion equations. *Physical Review E*, 65(4):041103, 2002.

[43] M. M. Meerschaert, J. Mortensen, and S. W. Wheatcraft. Fractional vector calculus for fractional advection–dispersion. *Physica A: Statistical Mechanics and its Applications*, 367:181–190, 2006.

[44] M. M. Meerschaert and A. Sikorskii. *Stochastic Models for Fractional Calculus*, volume 43. Walter de Gruyter, Berlin, 2012.

[45] M. M. Meerschaert and P. Straka. Inverse stable subordinators. *Mathematical Modelling of Natural Phenomena*, 8(2):1–16, 2013.

[46] M. M. Meerschaert and C. Tadjeran. Finite difference approximations for fractional advection–dispersion flow equations. *Journal of Computational and Applied Mathematics*, 172(1):65–77, 2004.

[47] M. M. Meerschaert and C. Tadjeran. Finite difference approximations for two-sided space-fractional partial differential equations. *Applied Numerical Mathematics*, 56(1):80–90, 2006.

[48] M. M. Meerschaert, Y. Zhang, and B. Baeumer. Tempered anomalous diffusion in heterogeneous systems. *Geophysics Research Letters*, 35(17):L17403, 2008.

[49] R. M. Neupauer and J. L. Wilson. Adjoint method for obtaining backward-in-time location and travel time probabilities of a conservative groundwater contaminant. *Water Resources Research*, 35(11):3389–3398, 1999.

[50] J. P. Nolan. Numerical calculation of stable densities and distribution functions. *Communications in Statistics. Stochastic Models*, 13(4):759–774, 1997.

[51] P. Paradisi, R. Cesari, F. Mainardi, and F. Tampieri. The fractional fick's law for non-local transport processes. *Physica A: Statistical Mechanics and its Applications*, 293(1):130–142, 2001.

[52] P. Patie and T. Simon. Intertwining certain fractional derivatives. *Potential Analysis*, 36(4):569–587, 2012.

[53] M. S. Phanikumar, I. Aslam, C. Shen, D. T. Long, and T. C. Voice. Separating surface storage from hyporheic retention in natural streams using wavelet decomposition of acoustic doppler current profiles. *Water Resources Research*, 43(5):W05406, 2007.

[54] I. Podlubny, A. Chechkin, T. Skovranek, Y. Chen, and B. M. V. Jara. Matrix approach to discrete fractional calculus ii: Partial fractional differential equations. *Journal of Computational Physics*, 228(8):3137–3153, 2009.

[55] G. Samoradnitsky and M. S. Taqqu. *Stable non-Gaussian Random Processes: Stochastic Models with Infinite Variance*, Volume 1. CRC Press, 1994.

[56] N. M. Schmadel, A. S. Ward, M. J. Kurz, J. H. Fleckenstein, J. P. Zarnetske, D. M. Hannah, T. Blume, M. Vieweg, P. J. Blaen, C. Schmidt, et al. Stream solute tracer timescales changing with discharge and reach length confound process interpretation. *Water Resources Research*, 52(4):3227–3245, 2016.

[57] R. Schumer, D. A. Benson, M. M. Meerschaert, and S. W. Wheatcraft. Eulerian derivation of the fractional advection–dispersion equation. *Journal of Contaminant Hydrology*, 48(1):69–88, 2001.

[58] R. Schumer, D. A. Benson, M. M. Meerschaert, and B. Baeumer. Fractal mobile/immobile solute transport. *Water Resources Research*, 39(10):1296, 2003.

[59] R. Schumer, D. A. Benson, M. M. Meerschaert and B. Baeumer. Multiscaling fractional advection-dispersion equations and their solutions. *Water Resources Research*, 39(1): 1022–1032, 2003.

[60] I. M. Sokolov and R. Metzler. Towards deterministic equations for Lévy walks: The fractional material derivative. *Physical Review E*, 67(1):010101, 2003.

[61] I. M. Sokolov and J. Klafter, From diffusion to anomalous diffusion: A century after Einstein's Brownian motion, *Chaos*, 15:026103, 2005.

[62] L. Wang and M. Cardenas. Non-Fickiantransport through two-dimensional rough fractures: Assessment and prediction. *Water Resources Research*, 50:871–884, 2014.

[63] G. Zaslavsky. Fractional kinetic equation for hamiltonian chaos. *Physica D: Nonlinear Phenomena*, 76(1-3):110–122, 1994.

[64] M. Zayernouri and G. E. Karniadakis. Fractional Sturm–Liouville eigenproblems: theory and numerical approximation. *Journal of Computational Physics*, 252:495–517, 2013.

[65] X. Zhang, J. W. Crawford, L. K. Deeks, M. I. Stutter, A. G. Bengough, and I. M. Young. A mass balance based numerical method for the fractional advection-dispersion equation: Theory and application. *Water Resources Research*, 41(7):W07029, 2005.

[66] X. Zhang, M. Lv, J. W. Crawford, and I. M. Young. The impact of boundary on the fractional advection–dispersion equation for solute transport in soil: Defining the fractional dispersive flux with the Caputo derivatives. *Advances in Water Resources*, 30(5):1205–1217, 2007.

[67] Y. Zhang, D. A. Benson, M. M. Meerschaert, and H.-P. Scheffler. On using random walks to solve the space-fractional advection-dispersion equations. *Journal of Statistical Physics*, 123(1):89–110, 2006.

[68] Y. Zhang, D. A. Benson, M. M. Meerschaert, and E. M. LaBolle. Space-fractional advection-dispersion equations with variable parameters: Diverse formulas, numerical solutions, and application to the macrodispersion experiment site data. *Water Resources Research*, 43(5):W05439, 2007.

[69] Y. Zhang, D. A. Benson, and D. M. Reeves. Time and space nonlocalities underlying fractional-derivative models: Distinction and literature review of field applications. *Advances in Water Resources*, 32(4):561–581, 2009.

[70] Y. Zhang, C. T. Green, E. M. LaBolle, R. M. Neupauer, and H. Sun. Bounded fractional diffusion in geological media: Definition and lagrangian approximation. *Water Resources Research*, 52:8561–8577, 2016.

[71] Y. Zhang, M. M. Meerschaert, and R. M. Neupauer. Backward fractional advection dispersion model for contaminant source prediction. *Water Resources Research*, 52(4):2462–2473, 2016.

[72] Y. Zhang, H.-G. Sun, R. M. Neupauer, and P. Straka. Identification of pollutant source using backward probability density functions for bounded super-diffusion. *Water Resources Research*, (in preparation), 2018.

[73] L. Zhou and H. Selim. Application of the fractional advection-dispersion equation in porous media. *Soil Science Society of America Journal*, 67(4):1079–1084, 2003.